J MATER SCI 41 (2006) 1691–1696

Microstructure and bonding properties of diffusion–bonded composite comprising an Fe–Al alloy and carbon steel

N. MASAHASHI*
Institute for Materials Research, Tohoku University, Katahira 2-1-1, Aoba, Sendai 980-8577, Japan
E-mail: masahasi@imr.tohoku.ac.jp

K. KOMATSU
Department of Materials Science, Graduate School, Tohoku University, Katahira 2-1-1, Aoba, Sendai 980-8577, Japan

S. WATANABE, S. HANADA
Institute for Materials Research, Tohoku University, Katahira 2-1-1, Aoba, Sendai 980-8577, Japan

Published online: 17 February 2006

This study discusses microstructure evolution, diffusion behavior and bonding strength of a couple comprising of an iron aluminium alloy (Fe–Al) and high carbon-steel (FeCMn) during diffusion bonding. A columnar microstructure evolves from the joint interface toward FeCMn and disappears in couples bonded for a long period. Aluminium diffusion from Fe–Al to FeCMn and columnar microstructure evolution are retarded as compared to a couple consisting of an Fe–Al and ferrite steel. The carbide in the FeCMn impedes the aluminium diffusion and retards the columnar grain evolution. When the carbide is dissolved in the ferrite during the aluminium diffsuion from Fe–Al, coarse grains evolve due to the coalescence of the columnar grains and a high-bonding strength is obtained. The hardness variation is minimum in the FeCMn of a couple bonded for a short period, which is explained by the microstructural changes in the columnar grain evolution and carbide dissociation.

1. Introduction

Iron–aluminium (Fe–Al) alloys possess attractive mechanical and chemical properties and have been considered as structural engineering materials for high temperature corrosion-resistant applications. The major drawbacks of these alloys are brittle fracture behaviour at ambient temperatures and a sharp drop in strength above 873 K [1]. The authors have proposed that composite laminates consisting of an Fe–Al alloy and a certain type of steel can provide the steel with additional properties, such as corrosion resistance, high strength, and light weight [2]. Laminated composites of an Fe–Al and steel have been fabricated by the clad rolling technique [3, 4]. They exhibit superior corrosion resistance in a dilute aqueous solution of H_2SO_4 at temperatures ranging from 313–373 K [5, 6] and in a chloride containing solution at 323 K [7].

On the other hand, fundamental properties such as microstructure evolution, diffusion behaviour, and bonding strength have been investigated using a diffusion couple consisting of an Fe–Al alloy and pure iron [2] or CrMo steel [3]. These properties demonstrate good bonding between the mating materials without the formation of an intermediate phase at the joint interface. Moreover, columnar grain evolution from the joint interface toward the steel side is observed in couples bonded at temperatures above A_3 (ferrite and austenite transformation temperature), which contributes to the bonding strength between the materials [2, 8]. The strengthening of the bonding is related to the alloying near the joint interface, which is accompanied by diffusion between the mating materials. On the other hand, the microstructure is also influenced by the diffusion in the present couple, because the mecha-

*Author to whom all correspondence should be addressed.
0022-2461
DOI: 10.1007/s10853-006-2934-y

TABLE I Summary of chemically analysed compositions in at% (conversion to wt.% in parentheses)

Sample	Fe	Al	Mn	C	O	N
FeCMn	97.3 (98.8)	–	0.83 (0.83)	1.89 (0.413)	0.0008	0.0003
16A1	84.4 (91.8)	15.6 (8.2)	–	0.01 (0.0013)	0.0005	<0.0001

Al and Mn were analyzed by ICP optical emission spectrometry.
C, O and N were analyzed by combustion-infrared absorption, helium gas-fusion infrared absorption and helium gas fusion-thermal conduction method, respectively.

nism of columnar microstructure evolution is understood by transformation in steel from gamma to alfa, which is caused by aluminum diffusion from an Fe–Al alloy to steel. Consequently, it is concluded that the bonding strength increases with the columnar microstructure evolution. These results are obtained by the diffusion bonding experiments performed using a couple of an Fe–Al alloy and ferrite steel. In this study, high-carbon steel was selected as the mating material of Fe–Al because it possesses high strength comparable to that of Fe–Al. As a result, the deformation resistance ratio approaches unity [9]. This feature is crucial to the fabrication of the composite based on the criterion, which considers the deformation resistance ratio, that different materials with metallurgical bonds should be deformed simultaneously [10]. Moreover, it is noteworthy that carbon steel is a commercially available low cost material that is used widely. This study aims at investigating the microstructure and diffusion behaviour of the couple of an Fe-Al alloy and high-carbon steel, and evaluating bonding properties. In particular, the influence of carbon or carbides in the carbon steel on the microstructure evolution and bonding is explored.

2. Experimental

The compositions of the Fe–Al alloy and the carbon steel are Fe–16at%Al (abbreviated as 16Al) and Fe–1.8at%C–0.9at%Mn (FeCMn), respectively. The composition of FeCMn is similar to that of commercially produced alloys. All the samples were prepared by argon arc melting, followed by hot rolling of 16Al at 1273 K and cold rolling of the FeCMn steel to 5 mm resulting in approximately 50% reduction. The Fe–Al alloy exhibits equiaxed coarse grains ranging from 300 μm to 1 mm while the FeCMn steel exhibits a deformation microstructure. A chemical analysis of as-cast ingots is presented in Table I. For diffusion bonding, specimens with dimensions of $5 \times 10 \times 10$ mm^3 were sectioned from the rolled plates using an electro-discharge machine, and the contact surfaces of the specimens were mechanically polished using a 1500 grade SiC paper and 1.0 μm alumina particles. The polished specimens were contacted by an alumina jig with the application of weak pressure. After diffusion bonding at 1323 K for 12, 48 and 192 h in a vacuum less than 2×10^{-3} Pa, the bonded couples were cooled in a furnace. Hereafter, the couple bonded for 12, 48 and 192 h will be referred to as 12, 48 and 192 DB, respectively.

All the bonded couples were cut into two pieces perpendicular to the joint interface, and their surfaces were mechanically polished using emery paper and alumina particles, followed by chemical polishing using a colloidal silica suspension with a particle size of 0.04 μm. One of the pieces was employed for microstructure observation, micro-Vickers measurement and SEM-EDX (FEI XL-30FEG) and EPMA analysis. Thin foils for the TEM observation using JEOL JEM3010 at 200 kV were prepared by electrochemical thinning at 15 V and 243–253 K in a twinjet polisher using a solution of 33% nitric acid

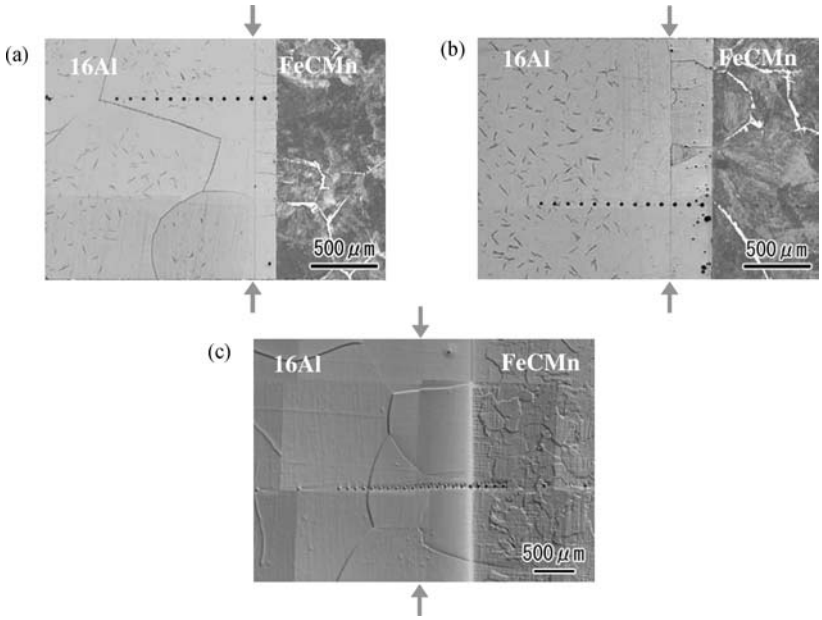

Figure 1 Optical micrographs of 12 DB (a), 48 DB (b) and 192 DB (c). Arrows indicate the joint interface.

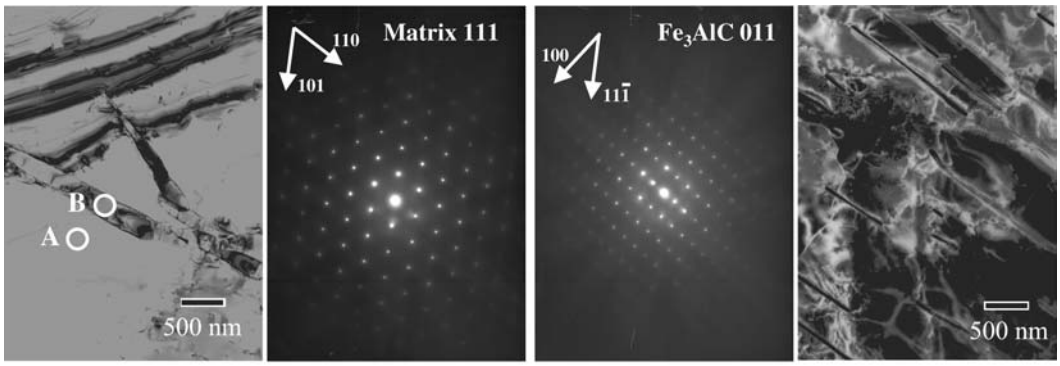

Figure 2 TEM images of the 16Al side (a) and FeCMn side (d) of 48 DB, and diffraction patterns of the matrix (b) and precipitate (c) obtained from the encircled regions A and B in (a).

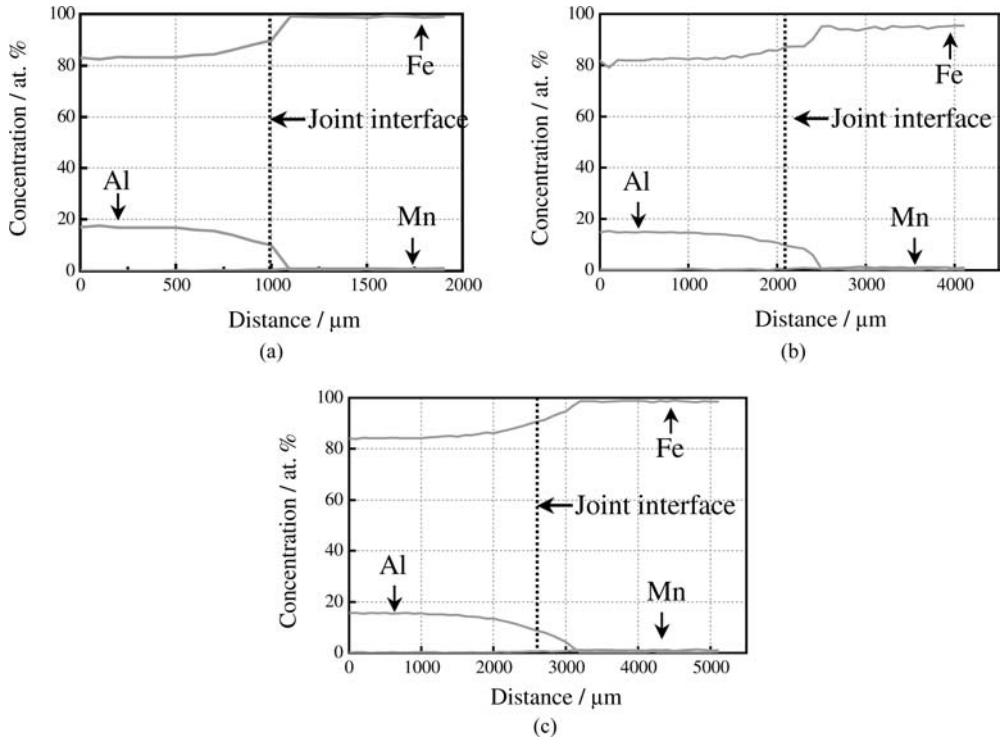

Figure 3 Concentration profiles of 12 DB (a), 48 DB (b) and 192 DB (c).

and methyl alcohol. The other piece was polished to a size of 5 × 5 × 10 mm^3 and subjected to a mechanical shear test at room temperature at a loading rate of 8.3 × 10^{-4} s^{-1}. The testing procedure is described in detail elsewhere [3].

3. Results

3.1. Microstructures

Fig. 1 shows the optical micrographs of 12 DB (a), 48 DB (b) and 192 DB (c). The columnar microstructure of 12 and 48 DB evolves from the joint interface toward the FeCMn side, while coarse grains across the joint interface are observed in 192 DB. While a second phase is not observed in 192 DB, it is observed in the FeCMn side beyond the columnar grains of 12 and 48 DB. On the other hand, acicular precipitates are observed in the 16Al side of 12 DB (a) and 48 DB (b), while they are not observed in that of 192 DB. Fig. 2 shows TEM images of the 16Al side (a) and FeCMn side (d) of 48 DB and diffraction patterns of the matrix (b) and precipitate (c) obtained from the encircled areas A and B in (a). From the diffraction pattern and TEM-EDX analysis, the precipitates were identified as Fe_3AlC with the pervoskite structure. This carbide has been reported by several papers [11, 12], and referred as the K phase [13]. The carbides of Fe_3C are observed in the FeCMn side of 48 DB in (d).

Fig. 3 shows the concentration profile of 12 DB (a), 48 DB, (b) and 192 DB (c). They exhibit continuous variations of the constituents between the mating materials without the formation of an intermediate phase. Fig. 4 shows the carbon map near the joint interface. In 12 DB

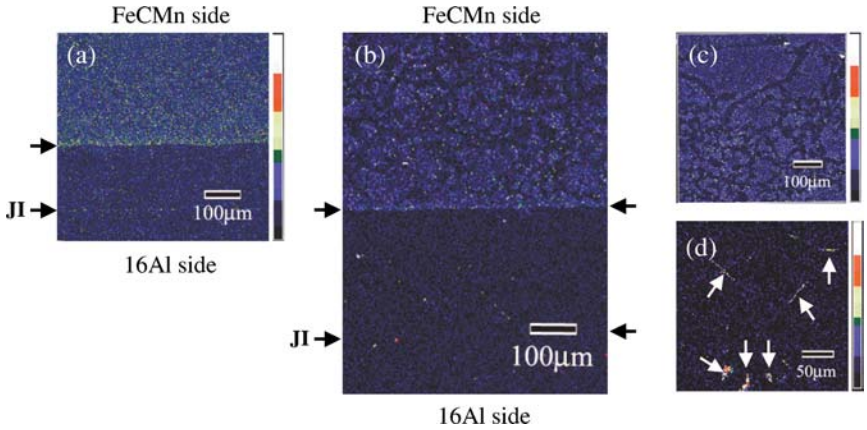

Figure 4 X-ray maps of carbon K_α in 12 DB (a), 48 DB (b) near the joint interface (JI), the FeCMn side of 48 DB (c), and the 16Al side of 48 DB (d). Arrows in (d) indicate the acicular precipitates.

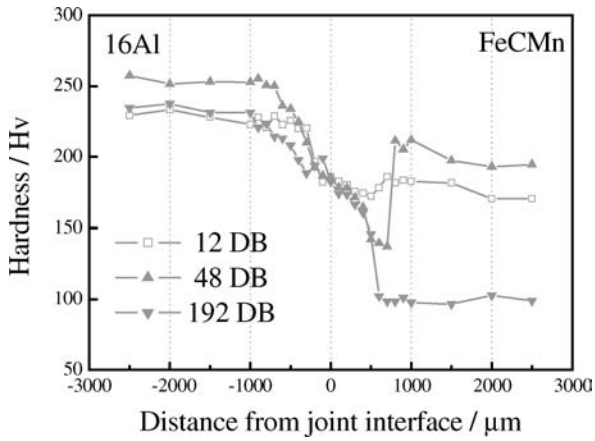

Figure 5 Hardness variations with respect to the distance from the joint interface of 12, 48 and 192 DB.

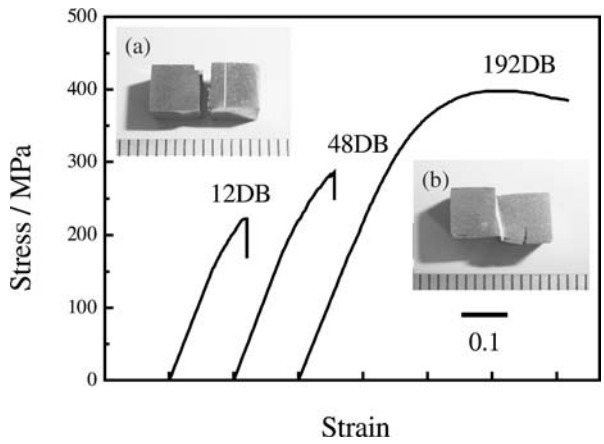

Figure 6 Shear stress-shear strain curves of 12, 48 and 192 DB.

(a), carbon is finely distributed in the FeCMn side and concentrated in a region approximately 130 μm from the joint interface. In 48 DB (b)(c), similar carbon concentration is observed at the region approximately 290 μm from the joint interface; however, the carbon concentration is low as compared to that in 12 DB. The low-carbon area is dispersed intricately in the FeCMn side of 48 DB. Acicular precipitates with carbon are observed in the 16Al sides of 12 and 48 DB (d). On the other hand, no salient characteristics of carbon distribution are observed in 192 DB.

3.2. Mechanical properties

Fig. 5 shows a plot of the variation of hardness against the distance from the joint interface. The hardness variation is minimum at approximately 500 and 700 μm from the joint interface in the FeCMn side of 12 and 48 DB, respectively. When as-rolled monolithic FeCMn is annealed at 1323 K for 12, 48 and 192 h, the average hardness values are 182, 197 and 205 Hv, respectively. These hardness values are close to those of FeCMn away from the joint interface of 12 and 48 DB. On the other hand, the hardness of the monolithic 16Al is 220 Hv irrespective of the annealing time, and it is lower than that of the 16Al matrix in the couples.

Fig. 6 shows the shear stress-strain curves. Both the bonding strength and strain to failure increase with an increase in the bonding time. The insets show the external views of 12 DB (a) and 192 DB (b) after the shear test. The mating materials of the 12 and 48 DB couples were separated after the maximum stress, while those of 192 DB remained intact with significant plastic deformation.

4. Discussion

In our previous paper, we have reported that the average length of the columnar grains and diffusion distance of aluminium increase with the bonding time [8]. The diffusion distance of aluminium is defined as the distance between the joint interface and the site wherein the aluminium concentration is zero in the concentration profile. In the present study, the diffusion distance of aluminium increases with the bonding time while the columnar microstructure of the couple bonded for 192 h disappears. Fig. 7 shows a plot of the average length of the columnar grains (a) and the diffusion distance of aluminium (b)

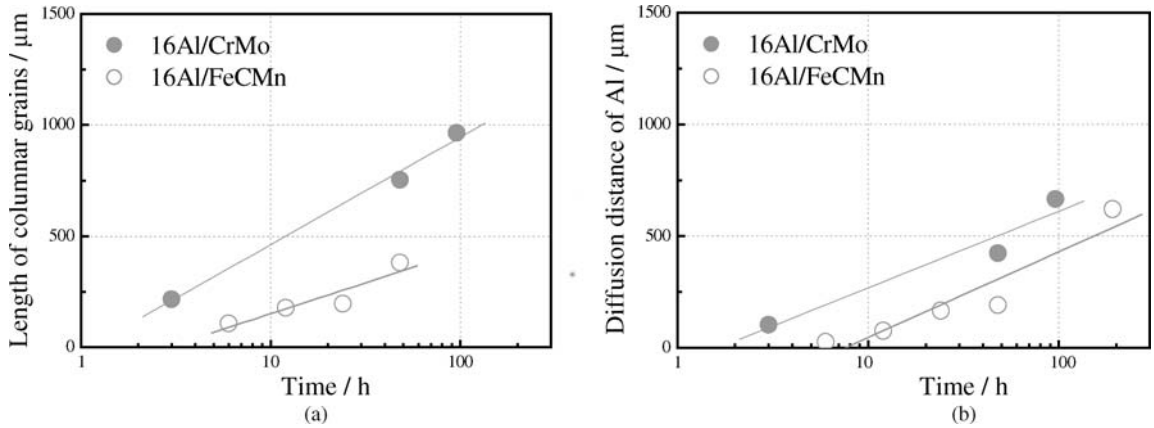

Figure 7 Dependence of the average length of the columnar grains (a) and diffusion distance of aluminium (b) on the annealing time.

against the bonding time. It includes additional experimental data of 6 and 24 DB (bonded at 1323 K for 6 and 24 h, respectively) and 16Al/CrMo (a couple of 16Al and CrMo steel bonded at 1323 K). The figure shows that the rate of increase in the diffusion distance of aluminium in 16Al/FeCMn is lower than that in 16Al/CrMo, and the growth rate of the columnar grain in 16Al/FeCMn is lower than that in 16Al/CrMo. This difference between both the couples is due to the constituent phases of steel: two phases of ferrite and carbide in FeCMn and only ferrite in CrMo. The evolution of the columnar grains is suppressed with a reduction in the interdiffusion coefficient [8]. By assuming that the carbide in FeCMn retards the aluminium diffusion, the transformation from gamma to ferrite should be retarded along with a delay in the nucleation of ferrite grains. The coalescence of the columnar grains observed in 192 DB could be explained by the suppression of the columnar grain evolution due to the retardation of the aluminium diffusion.

A local equilibrium of the quaternary system (Fe–Al–C–Mn) determines the state of carbon (in solution or carbides). The state and morphology depend on the bonding time and the position from the joint interface in the couple. The absence of the precipitates in 192 DB (Fig. 1c) is due to the dissolution of carbides into FeCMn, because carbon is soluble in the ferrite phase at equilibrium. Based on a recent study on phase equilibrium in the Fe–Al–C ternary system, the solubility of carbon in ferrites is up to 1.5at% [11]. By assuming that the carbon solubility in the ternary alloy is approximately the same as that in the Fe–Al–C–Mn system, carbon is dissociated near the joint interface at equilibrium. The initial two phases of ferrite and carbide in FeCMn are transformed to single phase of ferrite by alloying with aluminium during diffusion bonding. In the FeCMn side of 12 and 48 DB, the columnar microstructure evolution and carbide decomposition occur simultaneously. The hardness of the FeCMn side that consists of ferrite and carbide decreases with the bonding time due to the decomposition of carbide. However, the hardness of the FeCMn side that is located away from the joint interface possesses a high value because carbide decomposition does not occur. On the other hand, the hardness of the columnar grain in FeCMn depends on the aluminium concentration and decreases with the distance from the joint interface. Hence, minimum hardness appears in the FeCMn side of 12 and 48 DB. Further annealing leads to a homogeneous distribution of carbon at equilibrium and a continuous variation in the hardness between 16Al and FeCMn is obtained.

The separation of the mating materials of 12 and 48 DB after the shear test suggests that the bonding strength of these couples is low. This is due to the insufficient interdiffusion of both materials, which is caused by the microstructure of the FeCMn side in which the carbide impedes the aluminium diffusion from 16Al toward FeCMn, as discussed earlier. The maximum stress and the strain to failure increase when the carbide is dissociated by long-time annealing (192 DB). This result indicates that steel whose microstructure impedes the interdiffusion should be avoided as a mating material of Fe–Al.

5. Conclusions

The microstructure, diffusion behaviour, and bonding strength were investigated using a couple of an Fe–Al alloy (16Al) and high-carbon steel (FeCMn) bonded at 1323 K for 12 h (12 DB), 48 h (48 DB) and 192 h (192 DB). The main conclusions are as follows:

1. Columnar microstructure evolution from the joint interface to the FeCMn side is observed in 12 and 48 DB while coarse grains are observed across the joint interface in the FeCMn side of 192 DB.
2. The carbide is dispersed in the FeCMn side beyond the columnar grain of 12 and 48 DB while it is not observed in 192 DB. Acicular precipitates of Fe_3AlC are observed in the 16Al side of 12 and 48 DB while they are not observed in the corresponding side of 192 DB.
3. The hardness variations in the FeCMn side of 12 and 48 DB are minimum. This result is due to the microstruc-

tural variation of the columnar grain evolution and carbide dissociation during diffusion bonding.

4. The mating materials of 12 and 48 DB were separated after the shear test while those of 192 DB remain intact with significant plastic deformation.

5. The carbides in the FeCMn side suppress the aluminium diffusion from 16Al to FeCMn and retard the evolution of columnar grains. This results in a low bonding strength. When the carbides are dissolved in the ferrite by alloying with aluminium, the aluminium diffusion is promoted and a high bonding strength is obtained.

Acknowledgements

The authors gratefully acknowledge Mr. Hayasaka and Mr. Aoyagi for the TEM observation, Mr. Murakami for EPMA analysis and Mr. Endo, Mr. Usui, Mr. Ono and Mr. Sato for constructing the mechanical testing jigs. The assistance of Dr. Takada, Dr. Ashino, Mr. Konno and Mr. Sakamoto in chemical analysis is also gratefully acknowledged. N.M. would like to thank Toray Science Foundation for providing financially support to this study.

References

1. C. G. MCKAMEY, J. H. DEVAN, P. F. TORTORELLI and V. K. SIKKA, *J. Mater. Res.* **6** (1991) 1779.
2. N. MASAHASHI, N. KONDO and S. HANADA, *Ann. Chim Sci. Mat.* **27** (2002) S231.
3. N. MASAHASHI, S. WATANABE, N. NOMURA, S. SEMBOSHI and S. HANADA, *Intermetallics* **13** (2005) 717.
4. N. MASAHASHI, K. KOMATSU, S. WATANABE and S. HANADA, *J. Alloy Compd.* **379** (2004) 272.
5. N. MASAHASHI, G. KIMURA, M. OKU, K. KOMATSU, S. WATANABE and S. HANADA, *Corros. Sci.* 2005, accepted.
6. N. MASAHASHI, K. KOMATSU, G. KIMURA, S. WATANABE and S. HANADA, *Mater. Sci. Forum* **502** (2005) 379.
7. G. KIMURA, N. MASAHASHI, S. WATANABE and S. HANADA, in Collected Abstracts of the Fall Meeting of the Japan Inst. Metals, Akita, September 2004 (The Japan Inst. Metals, 2004) p. 284.
8. N. MASAHASHI and S. HANADA, *ISIJ Int.* **44** (2004) 878.
9. K. KOMATSU, N. MASAHASHI, S. WATANABE and S. HANADA, in Collected Abstracts of the Spring Meeting of the Japan Inst. Metals, Chiba, March 2003 (The Japan Inst. Metals, 2003) p. 260.
10. X. GOMEZ and J. ECHEBERRIA, *Mat. Sci. and Eng. A–Struct*, **348** (2003) 180.
11. P. VILLARS, A. PRINCE and H. OKAMOTO, in ''Handbook of Ternary Alloy Phase Diagrams Vol. 3 (ASM International, Materials Park, Ohio, 1995) p. 2850.
12. M. PALM and G. INDEN, *Intermetallics* **3** (1995) 443.
13. W. SANDERS and G. SAUTHOFF, *ibid.* **5** (1997) 361.

Received 19 April
and accepted 9 June 2005